CU/CoA-9309

Cranfield UNIVERSITY

Fully Discrete High-Order Schemes for Hyperbolic Conservation Law

J.Shi and E.F.Toro

COA report No.9309
December 1993

Department of Aerospace science
College of Aeronautics
Cranfield University
Cranfield, Bedford MK43 0AL, England

College of Aeronautics Report No. 9309
December 1993

Fully Discrete High-Order Schemes for Hyperbolic Conservation Laws

J.Shi and E.F.Toro

ISBN 1 871564 67 0

£10

Department of Aerospace Science
College of Aeronautics
Cranfield University
Cranfield, Bedford MK43 0AL, England

Cranfield
COA REPORT No. 9309
December, 1993

FULLY DISCRETE HIGH-ORDER SCHEMES FOR HYPERBOLIC CONSERVATION LAWS

J.Shi and E.F.Toro

DEPARTMENT OF AEROSPACE SCIENCE
COLLEGE OF AERONAUTICS
CRANFIELD UNIVERSITY
CRANFIELD, MK43 OAL, U.K.

Abstract

In this paper we investigate fully discrete high-order accurate solutions for system of hyperbolic conservation laws. Second-, third- and fourth-order high resolution schemes are presented. Performance of the methods is assessed by solving test problems for time-dependent Euler equations of Gas Dynamics in one and two space dimensions. We use exact solutions and experimental data to validate the results.

1 Introduction

An important research subject in Computational Fluid Dynamics (CFD) concerns the development of high-order numerical schemes. There are many application areas for which such research is of vital importance. One example of considerable interest is Acoustics, which needs long time evolution of weak flow features. For this kind of problems low-order methods will produce unacceptable dispersive and diffusive errors in a very short time. Another example concerns problems containing weak shocks in which the physical effects of diffusion and dispersion are important mechanisms. Low-order methods contain large amounts of numerical diffusion and dispersion and are thus totally inaccurate for simulating the propagation of weak shocks. In large computational problems low-order methods would require vast amounts of computer memory (possibly not available in current computers) in order to attain a satisfactory degree of accuracy. A high-order method would attain the same accuracy with coarser meshes requiring less sophisticated hardware and making it possible to actually run the problems.

Essentially, there are two different techniques to construct high-order numerical schemes: semi-discrete and fully discrete methods. In the semi-discrete method [1] one divides the discretization process into two separate stages. In the first stage one discretizes in space only leaving the problem continuous in time; in the second stage one has sets of Ordinary Differential Equations (ODE) in time, which can be discretized appropriately. Often this technique is called **the method of lines.** The MUSCL approach introduced by van Leer [2] can be utilised in conjunction with the method of lines. The recently developed ENO schemes [3]-[5] belong to this category. The main idea of the ENO scheme is that the spacial high-order approximations to the flux at a cell interface can be defined using high-order interpolation in space, and then the high-order temporal accuracy can be achieved by another discretization applying a high-order ODE solver.

In [6] Shi and Toro proposed a fully discrete technique to construct schemes of arbitrary accuracy and as examples presented fully discrete second-, third-, and fourth-order schemes for a linear model hyperbolic conservation law. In order to

prevent the spurious oscillations of the high-order methods when computing discontinuous solution, Total Variation Diminishing (TVD) constraints using flux limiters for fully discrete second-, third- and fourth-order schemes were introduced in [7].

In this paper we extend the previous works to general system of conservation laws. We first discuss linear systems and then extend the discussion to non-linear systems of conservation laws. To illustrate the methodology we present second-order, third-order and fourth-order schemes. Applications to the time-depent Euler equations in one and two dimensions are presented.

The rest of the paper is organized as follows: section 2 briefly reviews the fully discrete high-order schemes for the scalar case; section 3 extends the schemes to linear systems; section 4 discusses nonlinear systems, discusses the time dependent Euler equations of Gas Dynamics and present second-, third- and fourth-order solutions to the Euler equations. sections 5 reports the numerical experiments; section 6 draws conclusions.

2 Review of Fully Discrete Schemes

In this section we review the fully discrete second, third and fourth-order conservative schemes for the scalar initial-value problem (IVP)

$$\begin{aligned} U_t + F(U)_x &= 0 \quad -\infty < x < \infty, \quad t \geq 0 \\ U(x,0) &= U_0(x) \end{aligned} \tag{1}$$

Here, U is a conserved variable and $F(U)$ is the physical flux of the hyperbolic conservation law.

We discretize the computational half plane by choosing a uniform cell with a cell width $h = \Delta x$ and a time step $k = \Delta t$, and define the computational grid $x_j = jh, \quad t_n = nk$. We use U_j^n to denote the computed approximation to the exact solution $U(x_j, t_n)$ of equation (1).

The final form of our schemes can be written in a conservative form as

$$U_j^{n+1} = U_j^n - \frac{k}{h}\left(F_{j+\frac{1}{2}} - F_{j-\frac{1}{2}}\right) \tag{2}$$

The high-order numerical fluxes $F_{j+1/2}$ are outlined in the following subsections. The details can be found in [6] and [7].

2.1 Fully Discrete Second-order Scheme

Our second-order scheme for the scalar hyperbolic conservation law has numerical flux

$$F_{j+\frac{1}{2}} = \frac{1}{2}(F_j^n + F_{j+1}^n) - \frac{|a_{j+\frac{1}{2}}|}{2}\Delta U_{j+\frac{1}{2}} + \frac{|a_{j+\frac{1}{2}}|}{2}(1 - |c_{j+\frac{1}{2}}|)\Delta U_{j+\frac{1}{2}} \tag{3}$$

where $a_{j+1/2}$ is the intercell wave speed and $c_{j+1/2}$ is the corresponding Courant number

$$c_{j+1/2} = \frac{a_{j+1/2}\,k}{h} \tag{4}$$

$$\Delta U_{j+1/2} = U_{j+1} - U_j \tag{5}$$

The stability condition of the scheme applied to the scalar equation is $|c_{j+1/2}| \leq 1 \quad \forall\, j$.

The oscillation-free scheme satisfies a TVD constraint via flux limiter ϕ_j and is given by

$$F_{j+\frac{1}{2}} = \frac{1}{2}(F_j^n + F_{j+1}^n) - \frac{|a_{j+\frac{1}{2}}|}{2}\Delta U_{j+\frac{1}{2}} + \frac{|a_{j+\frac{1}{2}}|}{2}(1 - |c_{j+\frac{1}{2}}|)\Delta U_{j+\frac{1}{2}}\phi_j \tag{6}$$

Here $\phi_j = \phi_j(\theta_j)$ is a function of a "local flow parameter" θ_j

$$\theta_j = \frac{\Delta U_{j-1/2}}{\Delta U_{j+1/2}} \quad for \quad c_{j+1/2} > 0 \tag{7}$$

$$\theta_j = \frac{\Delta U_{j+3/2}}{\Delta U_{j+1/2}} \quad for \quad c_{j+1/2} < 0 \tag{8}$$

For convenience we repeat here two limiter functions. One is the FD2A (fully discrete second-order A)

$$\phi_j(\theta_j) = max\left[0, min\left(1, \frac{\theta_j}{\eta_{j+1/2}}\right), min\left(\theta_j, \frac{1}{\eta_{j+1/2}}\right)\right] \tag{9}$$

and the other is FD2B limiter

$$\phi_j(\theta_j) = max\left[0, min\left(1, \frac{2\theta_j}{\eta_{j+1/2}}\right), min\left(\theta_j, \frac{2}{\eta_{j+1/2}}\right)\right] \tag{10}$$

where

$$\begin{cases} \eta_{j+1/2} = 1 - |c_{j+1/2}| & for \quad 0 \le |c_{j+1/2}| < \frac{1}{2} \\ \eta_{j+1/2} = |c_{j+1/2}| & for \quad \frac{1}{2} \le |c_{j+1/2}| \le 1 \end{cases} \tag{11}$$

2.2 Fully Discrete Third-order Scheme

The five-point, third-order scheme has the numerical flux

$$\begin{aligned} F_{j+\frac{1}{2}} &= \frac{1}{2}\left(F_j^n + F_{j+1}^n\right) - \frac{|a_{j+\frac{1}{2}}|}{2}\Delta U_{j+\frac{1}{2}} + \left(|a_{j+\frac{1}{2}}| D_{j+\frac{1}{2}} \Delta U_{j+\frac{1}{2}}\right. \\ &\quad \left. + |a_{j+L+\frac{1}{2}}| D_{j+L+\frac{1}{2}} \Delta U_{j+L+\frac{1}{2}}\right)\phi_j \end{aligned} \tag{12}$$

Here

$$\begin{cases} D_{j+1/2} = \frac{1}{3} - \frac{1}{2}|c_{j+1/2}| + \frac{1}{6}c_{j+1/2}^2 \\ D_{j+L+1/2} = \frac{1}{6}(1 - c_{j+L+1/2}^2) \end{cases} \tag{13}$$

$$\Delta U_{j+L+1/2} = U_{j+L+1} - U_{j+L} \tag{14}$$

$$\begin{cases} L = -1 & if \; c_{j+1/2} > 0 \\ L = 1 & if \; c_{j+1/2} < 0 \end{cases} \tag{15}$$

Note that the stencil of this scheme is upwind biased.

Two third-order limiters are obtained from the following limiter

$$\begin{aligned} \phi_j &= \frac{(1-|c_{j+L+1/2}|)\theta_j}{\eta_{j+L+1/2}(D_{j+L+1/2}\theta_j + D_{j+1/2})} && if \quad 0 \le \theta_j < \theta^L \\ \phi_j &= 1 && if \quad \theta^L \le \theta_j \le \theta^R \\ \phi_j &= \frac{(1-|c_{j+L+1/2}|)}{\eta_{j+L+1/2}(D_{j+L+1/2}\theta_j + D_{j+1/2})} && if \quad \theta_j > \theta^R \\ \phi_j &= 0 && if \quad \theta_j \le 0 \end{aligned} \tag{16}$$

For the FD3A limiter

$$\theta^L = \frac{\eta_{j+L+1/2}\; D_{j+1/2}}{1 - |c_{j+L+1/2}| - \eta_{j+L}\; D_{j+L+1/2}} \tag{17}$$

$$\theta^R = \frac{1 - |c_{j+L+1/2}| - \eta_{j+L+1/2}\; D_{j+1/2}}{\eta_{j+L+1/2}\; D_{j+L+1/2}} \tag{18}$$

and for the FD3B limiter

$$\theta^L = 1.1\eta_{j+1/2} - 0.17 \tag{19}$$

$$\theta^R = 2.78 - 1.4\eta_{j+1/2} \tag{20}$$

The stability condition of the unlimited scheme applied to the scalar equation is $|c_{j+1/2}| \leq 1 \quad \forall\, j$.

2.3 Fully Discrete Fourth-order Scheme

The five-point, fourth-order numerical flux has the following form

$$\begin{aligned} F_{j+\frac{1}{2}} &= \frac{1}{2}(F_j^n + F_{j+1}^n) - \frac{|a_{j+\frac{1}{2}}|}{2}\Delta U_{j+\frac{1}{2}} \\ &+ \left(|a_{j+\frac{1}{2}}|\ D_{j+\frac{1}{2}}\Delta U_{j+\frac{1}{2}} + |a_{j+L+\frac{1}{2}}|\ D_{j+L+\frac{1}{2}}\Delta U_{j+L+\frac{1}{2}}\right)\ \phi_j \\ &+ |a_{j+M+\frac{1}{2}}|\ D_{j+M+\frac{1}{2}}\Delta U_{j+M+\frac{1}{2}}\ \phi_{j+M} \end{aligned} \tag{21}$$

Here

$$\begin{cases} D_{j+L+\frac{1}{2}} = \frac{1}{12} + \frac{1}{24}|c_{j+L+\frac{1}{2}}| - \frac{1}{12}c^2_{j+L+\frac{1}{2}} - \frac{1}{24}|c^3_{j+L+\frac{1}{2}}| \\ D_{j+\frac{1}{2}} = \frac{1}{2} - \frac{7}{12}|c_{j+\frac{1}{2}}| + \frac{1}{12}|c^3_{j+\frac{1}{2}}| \\ D_{j+M+\frac{1}{2}} = \frac{1}{12}c^2_{j+M+\frac{1}{2}} + \frac{1}{24}|c_{j+M+\frac{1}{2}}| - \frac{1}{12} - \frac{1}{24}|c^3_{j+M+\frac{1}{2}}| \end{cases} \tag{22}$$

$$\begin{cases} L = -1, \quad M = 1 \quad if\ \ c_{j+1/2} > 0 \\ L = 1, \quad M = -1 \quad if \quad c_{j+1/2} < 0 \end{cases} \tag{23}$$

This scheme has a centered stencil.

Two fourth-order limiters are obtained from the following limiters

$$\begin{aligned} \phi_j &= \frac{(1-|c_{j+L+1/2}|)\ \theta_j}{\eta_{j+L+1/2}(D_{j+L+1/2}\ \theta_j + D_{j+1/2} - D_{j+M+1/2})} && if \quad 0 \leq \theta_j < \theta^L \\ \phi_j &= 1 && if \quad \theta^L \leq \theta_j \leq \theta^R \\ \phi_j &= \frac{1-|c_{j+L+1/2}| + \eta_{j+L+1/2}\ D_{j+M+1/2}/\ \theta_j^*}{\eta_{j+L+1/2}(D_{j+L+1/2}\ \theta_j + D_{j+1/2})} && if \quad \theta_j > \theta^R \\ \phi_j &= 0 && if \quad \theta_j \ \ or \ \ \theta_j^* \leq 0 \end{aligned} \tag{24}$$

and

$$\begin{aligned} \phi_{j+M} &= \eta_{j+M+1/2}\ \theta_{j+M} \quad for \quad 0 \le \theta_{j+M} < \tfrac{1}{2} \\ \phi_{j+M} &= 1 \qquad\qquad\qquad for \quad \theta_{j+M} > \tfrac{1}{2} \\ \phi_{j+M} &= 0 \qquad\qquad\qquad for \quad \phi_j = 0 \end{aligned} \tag{25}$$

where for FD4A limiter

$$\theta^L = \frac{\eta_{j+L+\frac{1}{2}}(D_{j+1/2} - D_{j+M+1/2})}{1 - |c_{j+L+1/2}| - \eta_{j+L+1/2}\ D_{j+L+1/2}} \tag{26}$$

$$\theta^R = \frac{1 - |c_{j+L+\frac{1}{2}}| - \eta_{j+L+\frac{1}{2}}(D_{j+1/2} - D_{j+M+1/2}/\ \theta_j^*)}{\eta_{j+L+1/2}\ D_{j+L+1/2}} \tag{27}$$

for FD4B limiter

$$\theta^L = \eta_{j+1/2} \tag{28}$$

$$\theta^R = \frac{1 - |c_{j+L+\frac{1}{2}}| - \eta_{j+L+\frac{1}{2}}(D_{j+1/2} - D_{j+M+1/2}/\ \theta_j^*)}{\eta_{j+L+1/2}\ D_{j+L+1/2}} \tag{29}$$

the $\theta_j^* = \theta_j \theta_{j+M}$ we called "upwind-downwind flow parameter" which is given by

$$\theta_j^* = \frac{\Delta U_{j-1/2}}{\Delta U_{j+3/2}} \quad for \quad c_{j+1/2} > 0 \tag{30}$$

$$\theta_j^* = \frac{\Delta U_{j+3/2}}{\Delta U_{j-1/2}} \quad for \quad c_{j+1/2} < 0 \tag{31}$$

The stability condition of the unlimited scheme applied to the scalar equation is $|c_{j+1/2}| \le 1 \quad \forall\, j$.

3 Linear Hyperbolic Systems

3.1 Introduction

In this section we extend the scalar schemes (6), (12) and (21) to solve the IVP problem for linear hyperbolic systems with constant coefficients

$$\begin{aligned} U_t + AU_x &= 0 \\ U(x,0) &= U_0(x) \end{aligned} \tag{32}$$

where U is a column vector of m conserved variables, and A is an m by m constant matrix.

This is a system of conservation laws with the flux function $F(u) = AU$ which is hyperbolic if A is diagonalizable with real eigenvalues, i.e. the matrix A can be written as

$$A = R\Lambda R^{-1} \tag{33}$$

where Λ= diag $\left(\lambda^{(1)}, \lambda^{(2)}, \ldots, \lambda^{(m)}\right)$ is the diagonal matrix of eigenvalues of A and $R = \left(r^{(1)}, r^{(2)}, \ldots, r^{(m)}\right)$ is the matrix of right eigenvectors of A.

Equation (33) means $AR = R\Lambda$, that is

$$Ar^{(p)} = \lambda^{(p)} r^{(p)}, \quad p = 1, 2, \ldots, m \tag{34}$$

The natural way to extend the scalar schemes to linear systems is obtained by defining expressions for the flux differences $\Delta F_{j+1/2} = A\Delta U_{j+1/2}$. This can be done by diagonalizing the system, solving local Riemann problems with left and right states U_j^n and U_{j+1}^n, i.e.

$$U(x,0) = \begin{cases} U_j^n & x < 0 \\ U_{j+1}^n & x > 0 \end{cases} \tag{35}$$

and letting

$$\alpha_{j+1/2} = R_{j+1/2}^{-1} \Delta U_{j+1/2} \tag{36}$$

here $R_{j+1/2}$ is the matrix of right eigenvectors at the interface $j + 1/2$, which for the linear constant coefficient case is of course constant; $\alpha_{j+1/2}$ is called wave strength vector with components $\alpha_{j+1/2}^{(p)}$ $(p = 1, 2, \ldots, m)$ accross the $p - th$ wave traveling at speed $\lambda_{j+1/2}^{(p)}$ in the $(j + 1/2) - th$ intercell.

Then we have

$$\Delta U_{j+\frac{1}{2}} = \sum_{p=1}^{m} \alpha_{j+\frac{1}{2}}^{(p)} \; r_{j+\frac{1}{2}}^{(p)} \tag{37}$$

Since $F(U) = AU$, this leads to

$$\Delta F_{j+\frac{1}{2}} = A \, \Delta U_{j+\frac{1}{2}}$$

$$= \sum_{p=1}^{m} \alpha_{j+\frac{1}{2}}^{(p)} \; A \; r_{j+\frac{1}{2}}^{(p)}$$

$$= \sum_{p=1}^{m} \alpha_{j+\frac{1}{2}}^{(p)} \; \lambda_{j+\frac{1}{2}}^{(p)} \; r_{j+\frac{1}{2}}^{(p)} \tag{38}$$

The single jump $\Delta F_{j+1/2} = |a_{j+1/2}|\Delta U_{j+1/2}$ in the scalar schemes (6), (12) and (21) with the appropriate interpretation for $|a_{j+1/2}|$ is now substituted by a summation of jump (38), which gives a natural extension to linear systems with constant coefficients. Next we discuss the extension of scheme (6), (12) and (21).

3.2 Second-order Scheme for Systems

The numerical flux of the second-order scheme for systems is now

$$F_{j+\frac{1}{2}} = \frac{1}{2}(F_j + F_{j+1}) - \frac{1}{2}\sum_{p=1}^{m} |\lambda_{j+\frac{1}{2}}^{(p)}| \;\; \alpha_{j+\frac{1}{2}}^{(p)} \;\; r_{j+\frac{1}{2}}^{(p)}$$
$$+\frac{1}{2}\sum_{p=1}^{m} \left(1 - |c_{j+\frac{1}{2}}^{(p)}|\right) \;\; |\lambda_{j+\frac{1}{2}}^{(p)}| \;\; \alpha_{j+\frac{1}{2}}^{(p)} \;\; r_{j+\frac{1}{2}}^{(p)} \;\; \phi_j^{(p)} \tag{39}$$

Here

$$c_{j+1/2}^{(p)} = \frac{\lambda_{j+1/2}^{(p)} \;\; k}{h} \tag{40}$$

The FD2A limiter applied to each wave p is now

$$\phi_j^{(p)} = max\left[0, min\left(1, \frac{\theta_j^{(p)}}{\eta_{j+1/2}^{(p)}}\right), min\left(\theta_j^{(p)}, \frac{1}{\eta_{j+1/2}^{(p)}}\right)\right] \tag{41}$$

and the FD2B limiter is

$$\phi_j^{(p)} = max\left[0, min\left(1, \frac{2\theta_j^{(p)}}{\eta_{j+1/2}^{(p)}}\right), min\left(\theta_j^{(p)}, \frac{2}{\eta_{j+1/2}^{(p)}}\right)\right] \tag{42}$$

where

$$\theta_j^{(p)} = \frac{\alpha_{j-1/2}^{(p)}}{\alpha_{j+1/2}^{(p)}} \quad if \;\; c_{j+1/2}^{(p)} > 0 \tag{43}$$

$$\theta_j^{(p)} = \frac{\alpha_{j+3/2}^{(p)}}{\alpha_{j+1/2}^{(p)}} \quad if \;\; c_{j+1/2}^{(p)} < 0 \tag{44}$$

$$\begin{cases} \eta^{(p)}_{j+1/2} = 1 - |c^{(p)}_{j+1/2}| & for \quad 0 \le |c^{(p)}_{j+1/2}| < \frac{1}{2} \\ \eta^{(p)}_{j+1/2} = |c^{(p)}_{j+1/2}| & for \quad \frac{1}{2} \le |c^{(p)}_{j+1/2}| \le 1 \end{cases} \tag{45}$$

3.3 Third-order Scheme for Systems

The five-point, third-order scheme (12) for linear systems is

$$\begin{aligned} F_{j+\frac{1}{2}} &= \frac{1}{2}(F_j + F_{j+1}) - \frac{1}{2}\sum_{p=1}^{m} |\lambda^{(p)}_{j+\frac{1}{2}}| \;\; \alpha^{(p)}_{j+\frac{1}{2}} \;\; r^{(p)}_{j+\frac{1}{2}} \\ &\quad + \sum_{p=1}^{m} \Big[D^{(p)}_{j+\frac{1}{2}} \; |\lambda^{(p)}_{j+\frac{1}{2}}| \;\; \alpha^{(p)}_{j+\frac{1}{2}} \;\; r^{(p)}_{j+\frac{1}{2}} \\ &\quad + D^{(p)}_{j+L+\frac{1}{2}} \; |\lambda^{(p)}_{j+L+\frac{1}{2}}| \;\; \alpha^{(p)}_{j+L+\frac{1}{2}} \;\; r^{(p)}_{j+L+\frac{1}{2}} \Big] \phi^{(p)}_j \end{aligned} \tag{46}$$

where

$$D^{(p)}_{j+1/2} = \frac{1}{3} - \frac{1}{2}|c^{(p)}_{j+1/2}| + \frac{1}{6}(c^{(p)}_{j+1/2})^2 \tag{47}$$

$$D^{(p)}_{j+L+1/2} = \frac{1}{6}\left(1 - (c^{(p)}_{j+L+1/2})^2\right) \tag{48}$$

$$\begin{aligned} \phi^{(p)}_j &= \frac{(1-|c^{(p)}_{j+L+1/2}|)\;\theta^{(p)}_j}{\eta^{(p)}_{j+L+1/2}\;(D^{(p)}_{j+L+1/2}\;\theta^{(p)}_j + D^{(p)}_{j+1/2})} && if \quad 0 \le \theta^{(p)}_j < \theta^L \\ \phi^{(p)}_j &= 1 && if \quad \theta^L \le \theta^{(p)}_j \le \theta^R \\ \phi^{(p)}_j &= \frac{1-|c^{(p)}_{j+L+1/2}|}{\eta^{(p)}_{j+L+1/2}\;(D^{(p)}_{j+L+1/2}\;\theta^{(p)}_j + D^{(p)}_{j+1/2})} && if \quad \theta^{(p)}_j > \theta^R \\ \phi^{(p)}_j &= 0 && if \quad \theta^{(p)}_j \le 0 \end{aligned} \tag{49}$$

For the FD3A

$$\theta^L = \frac{\eta^{(p)}_{j+L+1/2}\; D^{(p)}_{j+1/2}}{1 - |c^{(p)}_{j+L+1/2}| - \eta^{(p)}_{j+L+1/2}\; D^{(p)}_{j+L+1/2}} \tag{50}$$

$$\theta^R = \frac{1 - |c^{(p)}_{j+L+1/2}| - \eta^{(p)}_{j+L+1/2}\; D^{(p)}_{j+1/2}}{\eta^{(p)}_{j+L+1/2}\; D^{(p)}_{j+L+1/2}} \tag{51}$$

and for the FD3B

$$\theta^L = 1.1\;\eta^{(p)}_{j+1/2} - 0.17 \tag{52}$$

$$\theta^R = 2.78 - 1.4\eta^{(p)}_{j+1/2} \tag{53}$$

with

$$\begin{cases} L=-1 & if \quad c^{(p)}_{j+1/2} > 0 \\ L=1 & if \quad c^{(p)}_{j+1/2} < 0 \end{cases} \tag{54}$$

3.4 Fourth-order Scheme for Systems

Following the examples above, the scalar fourth-order scheme (21) can be extended to linear hyperbolic systems in the same manner as

$$\begin{aligned} F_{j+\frac{1}{2}} &= \frac{1}{2}(F^n_j + F^n_{j+1}) - \frac{1}{2}\sum_{p=1}^{m} |\lambda^{(p)}_{j+\frac{1}{2}}| \;\; \alpha^{(p)}_{j+\frac{1}{2}} \;\; r^{(p)}_{j+\frac{1}{2}} \\ &+ \sum_{p=1}^{m} \Big(D^{(p)}_{j+\frac{1}{2}} \;\; |\lambda^{(p)}_{j+\frac{1}{2}}| \;\; \alpha^{(p)}_{j+\frac{1}{2}} \;\; r^{(p)}_{j+\frac{1}{2}} \\ &+ D^{(p)}_{j+L+\frac{1}{2}} \;\; |\lambda^{(p)}_{j+L+\frac{1}{2}}| \;\; \alpha^{(p)}_{j+L+\frac{1}{2}} \;\; r^{(p)}_{j+L+\frac{1}{2}} \Big) \phi^{(p)}_j \\ &+ D^{(p)}_{j+M+\frac{1}{2}} \;\; |\lambda^{(p)}_{j+M+\frac{1}{2}}| \;\; \alpha^{(p)}_{j+M+\frac{1}{2}} \;\; r^{(p)}_{j+M+\frac{1}{2}} \;\; \phi^{(p)}_{j+M} \end{aligned} \tag{55}$$

where

$$D^{(p)}_{j+L+1/2} = \frac{1}{12} + \frac{1}{24}|c^{(p)}_{j+L+1/2}| - \frac{1}{12}(c^{(p)}_{j+L+1/2})^2 - \frac{1}{24}|(c^{(p)}_{j+L+1/2})^3| \tag{56}$$

$$D^{(p)}_{j+1/2} = \frac{1}{2} - \frac{7}{12}|c^{(p)}_{j+1/2}| + \frac{1}{12}|(c^{(p)}_{j+1/2})^3| \tag{57}$$

$$D^{(p)}_{j+M+1/2} = \frac{1}{12}(c^{(p)}_{j+M+1/2})^2 + \frac{1}{24}|c^{(p)}_{j+M+1/2}| - \frac{1}{12} - \frac{1}{24}|(c^{(p)}_{j+M+1/2})^3| \tag{58}$$

The FD4 limiters are now

$$\begin{aligned} \phi^{(p)}_j &= \frac{(1-|c^{(p)}_{j+L+1/2}|)\;\theta^{(p)}_j}{\eta^{(p)}_{j+L+1/2}\;(D^{(p)}_{j+L+1/2}\;\theta^{(p)}_j + D^{(p)}_{j+1/2} - D^{(p)}_{j+M+1/2})} && if \quad 0 \le \theta^{(p)}_j < \theta^L \\ \phi^{(p)}_j &= 1 && if \quad \theta^L \le \theta^{(p)}_j \le \theta^R \\ \phi^{(p)}_j &= \frac{1-|c^{(p)}_{j+L+1/2}| + \eta^{(p)}_{j+L+1/2}\; D^{(p)}_{j+M+1/2}/\;\theta^{*(p)}_j}{\eta^{(p)}_{j+L+1/2}\;(D^{(p)}_{j+L+1/2}\;\theta^{(p)}_j + D^{(p)}_{j+1/2})} && if \quad \theta^{(p)}_j > \theta^R \\ \phi^{(p)}_j &= 0 && if \quad \theta^{(p)}_j \;\; or \;\; \theta^{*(p)}_j \le 0 \end{aligned} \tag{59}$$

$$\begin{aligned} \phi^{(p)}_{j+M} &= \eta^{(p)}_{j+M+1/2}\;\theta^{(p)}_{j+M} && for \quad 0 \le \theta^{(p)}_{j+M} < \tfrac{1}{2} \\ \phi^{(p)}_{j+M} &= 1 && for \quad \theta^{(p)}_{j+M} > \tfrac{1}{2} \\ \phi^{(p)}_{j+M} &= 0 && for \quad \phi^{(p)}_j = 0 \end{aligned} \tag{60}$$

For the FD4A limiter we have

$$\theta^L = \frac{\eta^{(p)}_{j+L+1/2}\,(D^{(p)}_{j+1/2} - D^{(p)}_{j+M+1/2})}{1 - |c^{(p)}_{j+L+1/2}| - \eta^{(p)}_{j+L+1/2}\,D^{(p)}_{j+L+1/2}} \tag{61}$$

$$\theta^R = \frac{1 - |c^{(p)}_{j+L+1/2}| - \eta^{(p)}_{j+L+1/2}\,(D^{(p)}_{j+1/2} - D^{(p)}_{j+M+1/2}/\theta^{*(p)}_j)}{\eta^{(p)}_{j+L+1/2}\,D^{(p)}_{j+L+1/2}} \tag{62}$$

and for the FD4B limiter

$$\theta^L = \eta^{(p)}_{j+1/2} \tag{63}$$

$$\theta^R = \frac{1 - |c^{(p)}_{j+L+1/2}| - \eta^{(p)}_{j+L+1/2}\,(D^{(p)}_{j+1/2} - D^{(p)}_{j+M+1/2}/\theta^{*(p)}_j)}{\eta^{(p)}_{j+L+1/2}\,D^{(p)}_{j+L+1/2}} \tag{64}$$

The upwind-downwind flow parameter is now

$$\theta^{*(p)}_j = \frac{\alpha^{(p)}_{j-1/2}}{\alpha^{(p)}_{j+3/2}} \quad if \quad c^{(p)}_{j+1/2} > 0 \tag{65}$$

$$\theta^{*(p)}_j = \frac{\alpha^{(p)}_{j+3/2}}{\alpha^{(p)}_{j-1/2}} \quad if \quad c^{(p)}_{j+1/2} < 0 \tag{66}$$

with

$$\begin{cases} L = -1, & M = 1 \quad if \quad c^{(p)}_{j+1/2} > 0 \\ L = 1, & M = -1 \quad if \quad c^{(p)}_{j+1/2} < 0 \end{cases} \tag{67}$$

4 Nonlinear Hyperbolic Systems

In this section we discuss the extension of the high-order schemes to nonlinear systems of conservation laws

$$U_t + F(U)_x + G(U)_y = 0 \tag{68}$$

where, $U(x,t)$ is column vector of m conserved variables; $F(U)$ and $G(U)$ are vector-valued, physical flux function of m components in x and y directions respectively.

The systems of equation (68) is assumed to be hyperbolic, that is all eigenvalues $\lambda^{(1)}(U), \lambda^{(2)}(U), \ldots, \lambda^{(m)}(U)$ of the m by m Jacobian matrix $A(U)$ and $B(U)$

$$A(U) = F'(U), \quad B(U) = G'(U) \tag{69}$$

are real for all U and there exists a complete set linearly independent corresponding right eigenvectors.

We take the Euler equations as a typical nonlinear system of conservation laws to develop the presentation on how to extend our schemes.

The two dimensional Euler equations of Gas Dynamics are

$$U = \begin{pmatrix} \rho \\ \rho u \\ \rho v \\ E \end{pmatrix}, \quad F(U) = \begin{pmatrix} \rho u \\ \rho u^2 + p \\ \rho uv \\ u(E+p) \end{pmatrix}, \quad G(U) = \begin{pmatrix} \rho u \\ \rho uv \\ \rho v^2 + p \\ v(E+p) \end{pmatrix} \tag{70}$$

$$p = (\gamma - 1)\left(E - \frac{1}{2}\rho(u^2 + v^2)\right) \tag{71}$$

here ρ, u, v, ρu, ρv, p, and E are the density, x and y direction velocitis, x and y direction momenta, pressure, and total energy respectively; the γ is the ratio of specific heats.

For the split one dimensional problem the eigenvalues of the Jocabean matrix $F'(U)$ are

$$\lambda^{(1)} = u - a, \quad \lambda^{(2)} = \lambda^{(3)} = u, \quad \lambda^{(4)} = u + a \tag{72}$$

The corresponding right eigenvectors are

$$r^{(1)} = \begin{pmatrix} 1 \\ u - a \\ v \\ h - ua \end{pmatrix}, \; r^{(2)} = \begin{pmatrix} 1 \\ u \\ v \\ \frac{1}{2}(u^2 + v^2) \end{pmatrix}, \; r^{(3)} = \begin{pmatrix} 0 \\ 0 \\ 1 \\ v \end{pmatrix}, \; r^{(4)} = \begin{pmatrix} 1 \\ u + a \\ v \\ h + ua \end{pmatrix} \tag{73}$$

where h is the specific enthalpy

$$h = \frac{E + p}{\rho} \tag{74}$$

The eigenvalues of the Jocabian matrix $G'(U)$ has the same form but the roles of u and v are interchanged.

There are essentially two ways of obtaining an intercell flux $F_{j+1/2}$ utilising a Riemann problem solution. One way is to obtain the flux function directely. For nonlinear systems this is always an approximate procedure. We called this the flux Riemann problem approach. Another way is to find the solution of the Riemann problem for the state variables $W_{j+1/2}$ and then the intercell flux can be obtained by evaluating the physical flux function, i.e. $F_{j+1/2} = F(W_{j+1/2})$. The solution $W_{j+1/2}$ can be approximate or exact. We call this the state Riemann problem approach.

4.1 Flux Riemann Solvers

A possible strategy for solving systems of nonlinear conservation laws is to linearize the nonlinear system of equations (68) locally at each cell interface by an approximate Riemann solver and then implement the methods of last section using the linearized systems

$$U_t + \bar{A}\, U_x \;=\; 0 \tag{75}$$

Here $\bar{A}$ is a linearized constant matrix depending only on the local data U_j^n and U_{j+1}^n, that is $\bar{A} = \bar{A}(U_j^n, U_{j+1}^n)$.

Popular examples of this approach are Roe's Riemann solver [8] and Osher's Riemann solver [9]. Roe's matrix $\bar{A}(U_j^n, U_{j+1}^n)$ is assumed to satisfy the following properties: (i) $\bar{A}\ \Delta U_{j+1/2} = \Delta F_{j+1/2}$; (ii) $\bar{A}$ is diagonalizable with real eigenvalues; (iii) $\bar{A} \rightarrow f'(\bar{U})$ smoothly as $U_j^n,\ U_{j+1}^n \rightarrow \bar{U}$. denoting the Roe eigenvalues, eigenvectors and wave strength as $\bar{\lambda}_{j+1/2}^{(p)}$, $\bar{r}_{j+1/2}^{(p)}$ and $\bar{\alpha}_{j+1/2}^{(p)}$ $(p = 1, 2, \ldots, m)$ then applying the high-order schemes of last section we solve the original nonlinear systems in a straight-forward manner.

The Roe eigenvalues and eigenvectors are evaluated at the average state $\bar{U}$ which

for the one-dimensional case takes the following form

$$\begin{cases} \bar{u} = (\rho_j^{1/2} u_j + \rho_{j+1}^{1/2} u_{j+1})/(\rho_j^{1/2} + \rho_{j+1}^{1/2}), & \bar{\rho} = (\rho_j \rho_{j+1})^{1/2} \\ \bar{h} = (\rho_j^{1/2} h_j + \rho_{j+1}^{1/2} h_{j+1})/(\rho_j^{1/2} + \rho_{j+1}^{1/2}), & \bar{a} = ((\gamma - 1)(\bar{h} - \frac{1}{2}\bar{u}^2))^{1/2} \end{cases} \tag{76}$$

The average wave strengths $\bar{\alpha}^{(p)}$ are determined by

$$\begin{cases} \bar{\alpha}^{(1)} = \frac{1}{2\bar{a}^2}(\Delta p - \bar{\rho}\bar{a}\Delta u) \\ \bar{\alpha}^{(2)} = \Delta\rho - \frac{\Delta p}{\bar{a}^2} \\ \bar{\alpha}^{(3)} = \frac{1}{2\bar{a}^2}(\Delta p + \bar{\rho}\bar{a}\Delta u) \end{cases} \tag{77}$$

here

$$\Delta\rho = \rho_{j+1} - \rho_j, \quad \Delta u = u_{j+1} - u_j, \quad \Delta p = p_{j+1} - p_j \tag{78}$$

However it is well known that under some circumstances Roe's Riemann solver can admite non-physical solutions, such as expansion shocks and negative densities. The first failure is due to the fact that Roe's Riemann solver does not satisfy an entropy condition [10]. To remedy this a sonic fix is required. There are several entropy fixes in the literature. In this paper we apply one introduced by Harten and Hyman [11]. The second failure afflicts all linearized Riemann solvers. Possible cures to this difficulty were studied by Roe etc. in [12].

A different approach to avoid compromising accuracy and robustness when using approximate Riemann solvers was proposed by Toro [13]. He proposed a hybrid approach in which a very simple linearised solver and an exact Riemann solver are used adaptively.

4.2 State Riemann Solvers

These solvers include exact solvers and hybrid solver which solve the Riemann problem for the state variables. Taking Toro's hybrid solver [13] for example. The hybrid solver includes a linearized solver and an exact solver which are used adaptively. The switch between the two solvers is governed by a simple mechanism. Applications of the solver shows that about 98 percent of all Riemann problems are solved by the fast linearized solver and only in the case of energetic flows the exact solver takes

over. The structure of the solution of the Riemann problem contains two intermediate regions between the two nonlinear waves. They are separated by the contact wave and we use the notation q_L^* and q_R^* for quantities to the left and right of the contact respectively.

The 'star values' obtained locally by the linearized solver in one dimension has the following form

$$\begin{cases} u^* = \frac{1}{2}(u_j + u_{j+1}) - (p_{j+1} - p_j)/2\bar{\rho}\bar{a} \\ p^* = \frac{1}{2}(p_j + p_{j+1}) - \frac{1}{2}\bar{\rho}\bar{a}(u_{j+1} - u_j) \\ \rho_L^* = \rho_j + (u_j - u^*)\bar{\rho}/\bar{a} \\ \rho_R^* = \rho_{j+1} + (u^* - u_{j+1})\bar{\rho}/\bar{a} \end{cases} \tag{79}$$

where

$$\bar{\rho} = \frac{1}{2}(\rho_j + \rho_{j+1}), \quad \bar{a} = \frac{1}{2}(a_j + a_{j+1}) \tag{80}$$

are the average values of the desity and sound speed.

Once the 'star values' at each cell interface are calculated the flux jump $\Delta F_{j+1/2}^{(p)}$ for each wave can be easily defined. Then applying the high-order schemes of last section we solve the nonlinear systems to high-order of accuracy. Note that in this approach the flux jump $\Delta F_{j+1/2}^{(p)}$ in the high order schemes is constructed directely, that is

$$\lambda_{j+\frac{1}{2}}^{(p)} \quad \alpha_{j+\frac{1}{2}}^{(p)} \quad r_{j+\frac{1}{2}}^{(p)} = \Delta F_{j+\frac{1}{2}}^{(p)} \tag{81}$$

5 Numerical Experiments

In this section we report numerical experiments with fully discrete second-order scheme (39), third-order scheme (46) and fourth-order scheme (55). The test problems are considered here as the follows:

5.1 Entropy Test Problem

Here we choose an entropy test problem with initial data

$$\begin{cases} (\rho,\ u,\ p) = (1,\ 0.75,\ 1) & 0 \leq x \leq 0.5 \\ (\rho,\ u,\ p) = (0.125,\ 0,\ 0.1) & 0.5 < x \leq 1.0 \end{cases} \tag{82}$$

This problem is a modification of Sod's problem and designed to produce a left sonic rarefaction about $x = 0.5$. Therefore it is a good problem to test the entropy-satifying property of a numerical scheme. Figure 1 and 2 show the performance of these schemes. The computational domain is devided by 100 computational cells. The Courant number used is 0.8. The solid line is the exact solution and the symbol is the numerical result. Figures 1 (a) (b) and (c) show the results obtained by the second-, third- and fourth-order schemes respectively with Roe's solver without entropy fix. As clearly shown the second-order scheme (a) automatically satisfies the entropy condition, whereas the solutions of the third- and fourth-order schemes (b) and (c) contain a rarefaction shock which is unphysical. Figure 2 shows the corresponding results obtained with Harten and Hyman's entropy fix [11]. The entropy-satisfying condition of the third- and fourth-order schemes is obviously improved.

(Fig. 1, 2 here)

5.2 Sod's Problem

The Sod's problem [16] is one of the most popular test problems for numerical schemes. Therefore we chose this problem to test all of our limiters presented in the previous sections. Sod's problem consists of initial data:

$$\begin{cases} (\rho,\ u,\ p) = (1,\ 0,\ 1) & 0 \leq x \leq 0.5 \\ (\rho,\ u,\ p) = (0.125,\ 0,\ 0.1) & 0.5 < x \leq 1.0 \end{cases} \tag{83}$$

Figures 3 to 8 show the comparison between the computed results (symbol) and the exact solution (line) with Roe's Riemann solver at time 0.2 units. Again we used

100 cells and 0.8 for the Courant number. Figure 3 shows the performance of the second-order scheme with the FD2A limiter. As seen in the figure the numerical results look satisfactory in the smooth parts. The shocks are captured with 2-3 interior points but the contact discontinuities are smeared with 4-5 points. There are no overshoots/undershoots.

Figure 4 shows the results of the second-order scheme with the FD2B limiter. Comparing with the resultd obtained by the FD2A (see Fig. 3) the FD2B has an obvious improvement of capturing the contact with 2-3 points, however there are overshoots and undershoots especially in internal energy plot (d).

Figure 5 shows the results obtained by the third-order scheme with the FD3A limiter. The results look very satisfactory for both smooth parts and shocks. But the contact has 4-5 points and there is a very little overshoots in the energy (d).

Figure 6 shows the performance of the third-order scheme with the FD3B limiter. Except for a little overshoots and undershoots the results of the limiter are very satisfactory. Both shocks and contacts are captured with only 2 points. The overall performance of the third-order scheme is superior to that of the second-order scheme (compare Fig. 5 and 6 with Fig. 3 and 4).

Figure 7 shows the numerical results of the fourth-order scheme with the FD4A limiter. The smooth part of the solution is good; shocks are captured with 3 points and the contacts with 5 points. Very small oscillations can be seen. However, it is generally accepted that designing proper dissipation procedure for high-order methods is a very difficulty tasks. We are satisfied with the performance observed.

Figure 8 shows the solution of the fourth-order scheme with the FD4B limiter. The results are nearly identical to that obtained by the FD4A (see Fig. 7) but the FD4B limiter is simpler than the FD4A.

(Fig. 3 to 8 here)

5.3 Blast-wave Problem

The blast-wave problem introduced by Woodward and Collela [17] is a severe test problem, therefore a good problem to test the robustness of numerical schemes. This problem has initial data:

$$\begin{cases} (\rho,\ u,\ p) = (1,\ 0,\ 1000) & 0 \leq x < 0.1 \\ (\rho,\ u,\ p) = (1,\ 0,\ 0.1) & 0.1 \leq x < 0.9 \\ (\rho,\ u,\ p) = (1,\ 0,\ 100) & 0.9 \leq x \leq 1.0 \end{cases} \tag{84}$$

Although there is no exact solution for this test problem there are several good numerical results available. We discretize the domain with 3000 cells. The Courant number used is 0.8. We applied a hybrid scheme involving Roe's solver and an exact solver used adaptively. We chose the second-order scheme with the FD2B, third-order with the FD3B and fourth-order with the FD4B to test the robustness of the high-order schemes. Figure 9 to 11 show the numerical results at time 0.028. The results show that schemes reproduce accurately the known features of the solution.

(Fig. 9 to 11 here)

5.4 Shock Reflection Problem

To illustrate the capability of our schemes to solve multi-dimensional problems we computed solutions to the time dependent, two-dimensional, Euler equations that simulate the flow that results from the reflection of shock wave at Mach number 1.7 from a wedge at an angle of 25 degree to the incident flow. A hybrid scheme involving the linearized solver and an exact solver used adaptively was applied. Figure 12 shows a comparison between the numerical solutions obtained by second-order with the FD2A limiter (a), third-order with the FD3A limiter (b), fourth-order with the FD4A limiter (c) and the experimental result (d) (Courtesy of Professor K. Takayama, Shock Wave Research Center, Tohoku University, Sendai, Japan). These results show a good agreements between the numerical and the experimental results.

(Fig. 12 here)

6 Conclusions

In this paper we discussed the way to extend scalar fully discrete high-order schemes to systems of conservation laws. Second-, third-, and fourth-order TVD schemes for nonlinear systems are presented. These schemes are tested and validated by solving the one and two dimensional Euler equations of Gas Dynamics for some well known test problems. The computation was carried out using two different kinds of approximate Riemann solvers which satisfy the entropy condition. The numerical solutions show that these high resolution schemes can give very satisfactory performance.

References

[1] **LEVEQUE, R.J.**, Numerical Methods for Conservation Laws. Birkhauser, 1990.

[2] **VAN LEER, B.**, Towards the Ultimate Conservative Difference Scheme. 2(1974), 3(1977), 4(1977), 5(1979), J. Comput. Phys., 1974-1979.

[3] **HARTEN, A. and OSHER, S.**, Uniformly High-order Accurate Non-oscillatory Schemes 1. SIAM J. Num. Anal., 24, pp. 279-309, 1987.

[4] **SHU, S. and OSHER, S.**, Efficient Implementation of Essentially Non-oscillatory Shock Capturing Schemes. J. Comput. Phys., 77, pp. 439-471, 1988.

[5] **HARTEN, A.**, ENO Schemes with Subcell Resolution. J. Comput. Phys., 83, pp. 148-184, 1989.

[6] **SHI, J. and TORO, E.F.**, Fully Discrete High-order Schemes for a Scalar Hyperbolic Conservation Law. COA Report No. 9307, Cranfield Institute of Technology, Cranfield, U.K., 1993.

[7] **SHI, J. and TORO, E.F.**, Fully Discrete High-order TVD Schemes for Scalar Hyperbolic Conservation Law, COA Report No. 9308, Cranfield Institute of Technology, Cranfield, U.K., 1993.

[8] **ROE, P.L.**, Approximate Riemann Solvers, Parameter Vectots, and Difference Schemes, J. Comput. Phys., 43(1981), pp.357-372.

[9] **ENGQUIST, B. and OSHER, S.**, One-side Difference Approximations for Nonlinear Conservation Laws, Mathematics of Computation, 36, 321-52, 1981.

[10] **ROE, P.L.**, Some Contributions to Modelling of Discontinuous Flows, Lectures in Applied Mathematics, Vol. 22, Am. Math. Soc., 1985.

[11] **HARTEN, A. and HYMAN, J.M.**, Self-adjusting grid methods for One-dimensional Hyperbolic Conservation Laws, J. Comput. Phys., 50(1983), pp. 235-269.

[12] **EINFELDT, B., MUNZ, C.D., ROE, P.L. and SJOGREEN, B.**, On Godnov-type Methods Near Low Densities, J. Comput. Phys., 92, 273-295, 1991.

[13] **TORO, E.F.**, A Linearized Riemann Solver for the Time Dependent Euler Equations of Gas Dynamics, Proc. R. Soc. Lond. A 434 pp 683-693, 1991.

[14] **TORO, E.F., Spruce, M., and Speares, W.**, Restoration of the Contact Surface in the HLL Riemann Solver, COA Report No. 9202, Cranfield Institute of Technology, Cranfield, U.K., 1992.

[15] **STRANG, G.**, Accurate Partial Differance Methods 2: Nonlinear Problem, SIAN J. Num. Anal., 5(1968), pp. 506-517.

[16] **SOD, G.**, A Survey of Several Finite Difference Methods for Systems of Non-linear Hyperbolic Conservation Laws, J. Comput. Phy., 27(1978), pp. 1-31.

[17] **WOODWARD, P. and COLELLA, P.**, The Numerical Simulation of Two-dimensional Fluid Flow with Strong Waves, J. Comput. Phys., 54, 115-173, 1984.

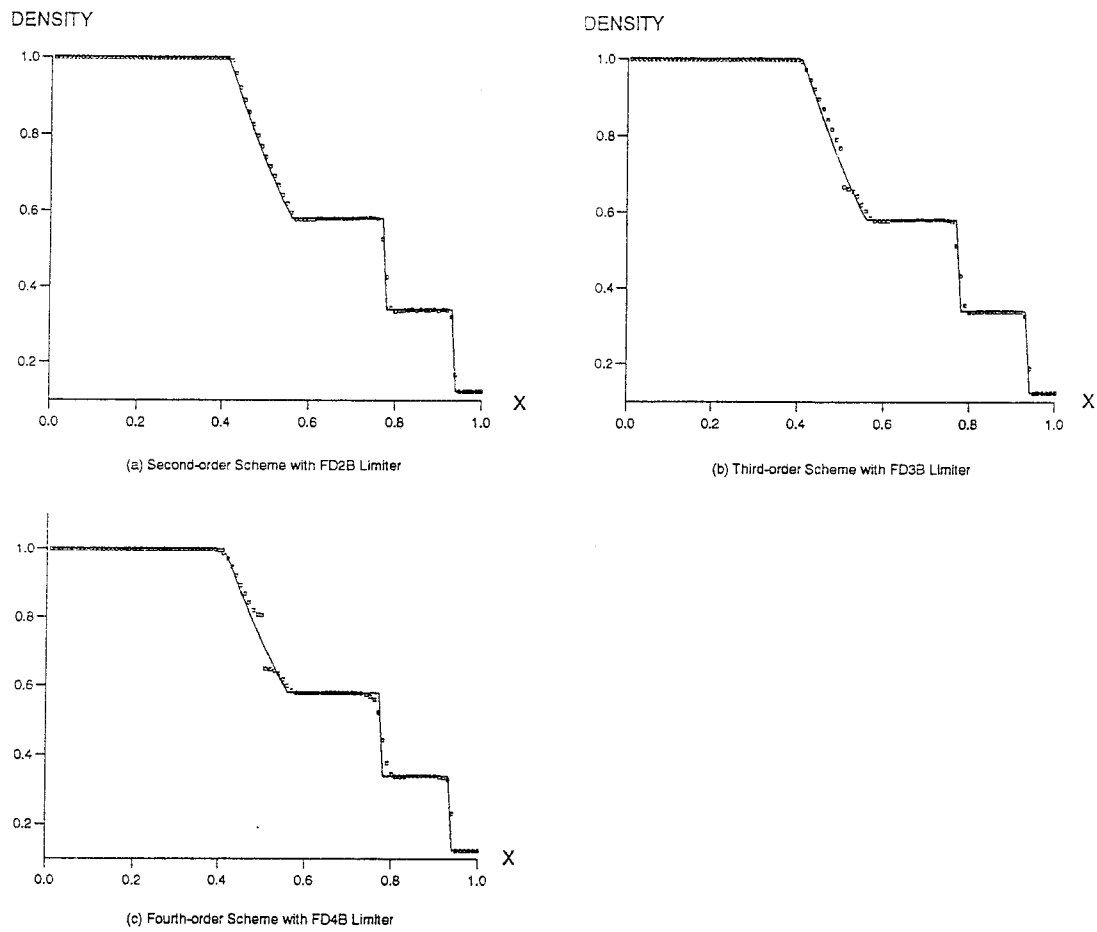

Figure 1: Entropy Test Problem without Entropy-fixing by the Second-, Third- and Fourth-order Schemes

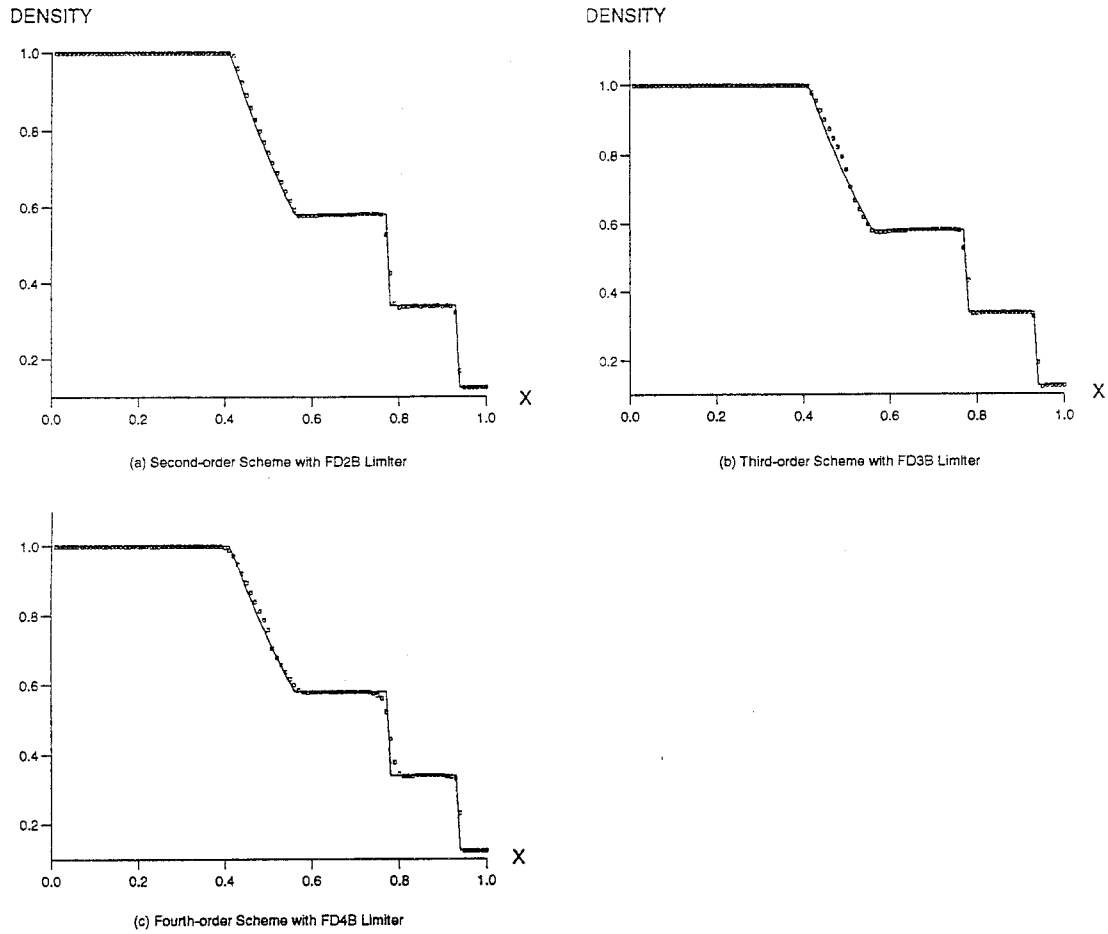

Figure 2: Entropy Test Problem with Entropy-fixing by the Second-, Third- and Fourth-order Schemes

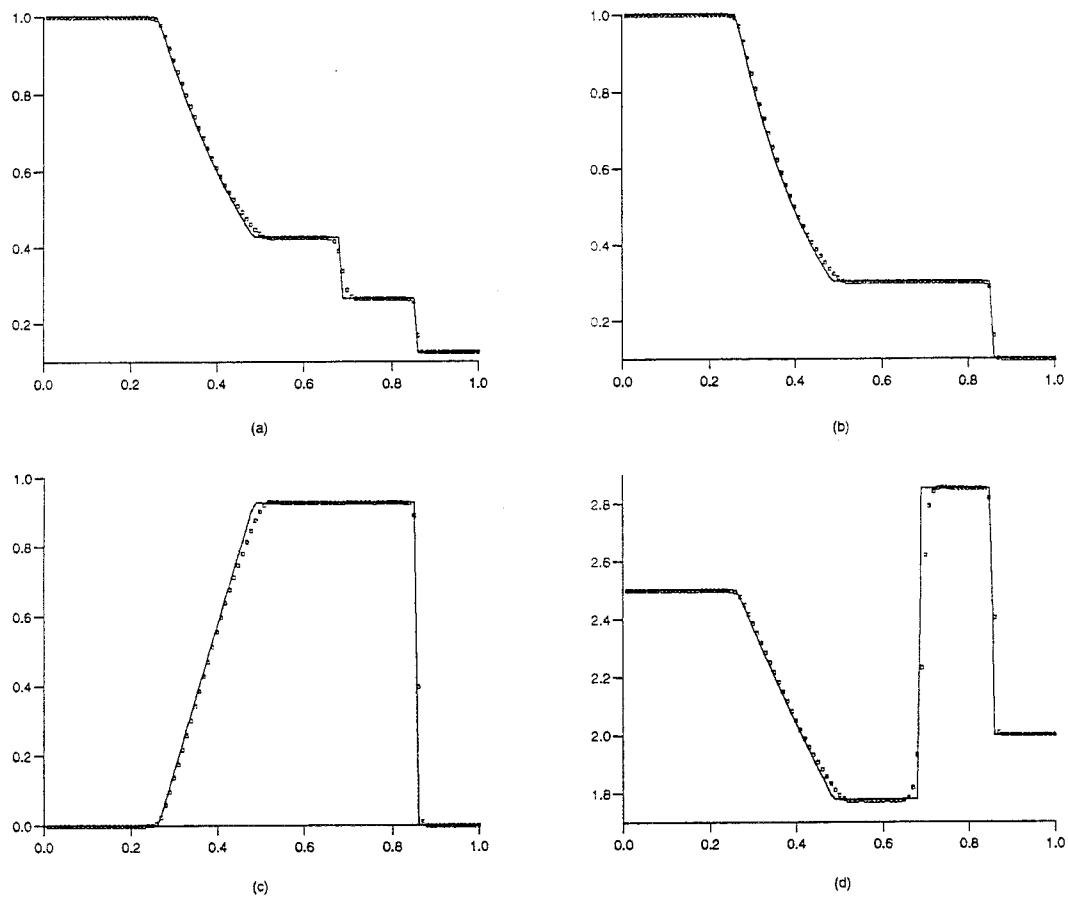

Figure 3: Sod's Problem by the Second-order Scheme with the FD2A Limiter: (a) Density, (b) Pressure, (c) Velocity, (d) Energy

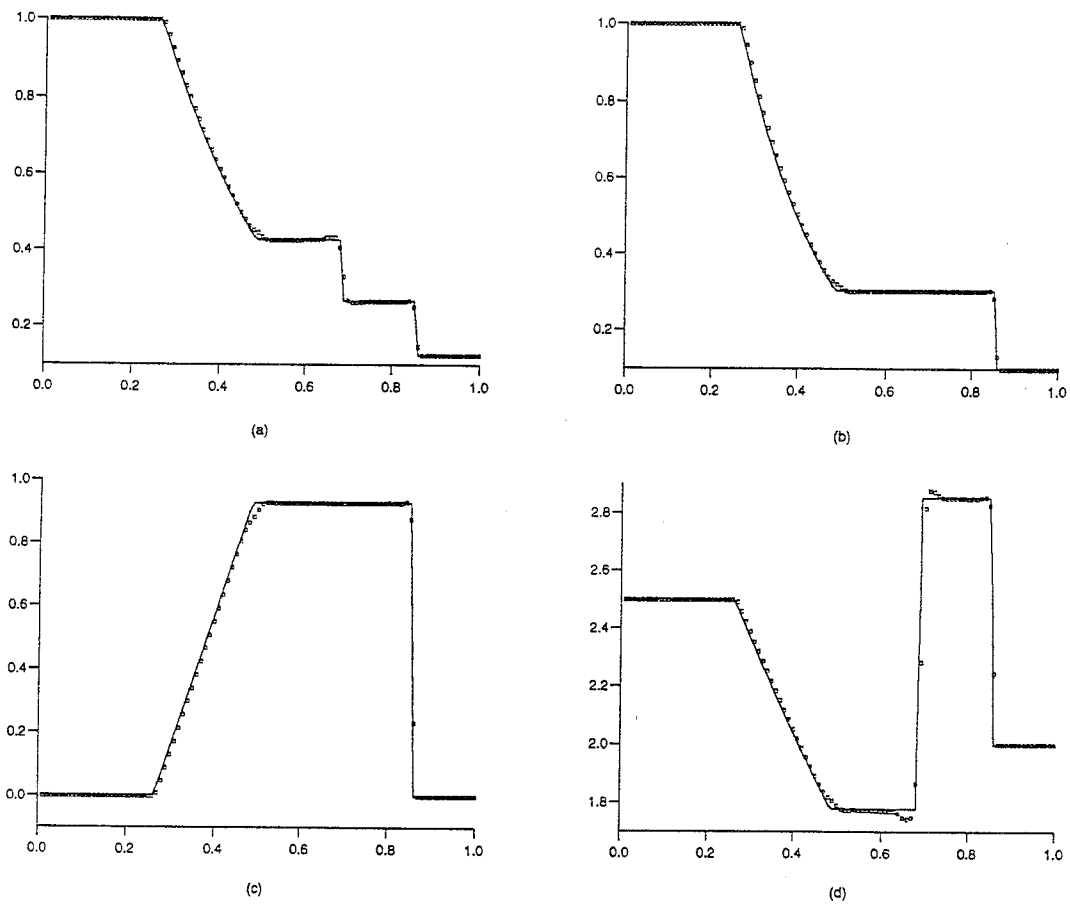

Figure 4: Sod's Problem by the Second-order Scheme with the FD2B Limiter: (a) Density, (b) Pressure, (c) Velocity, (d) Energy

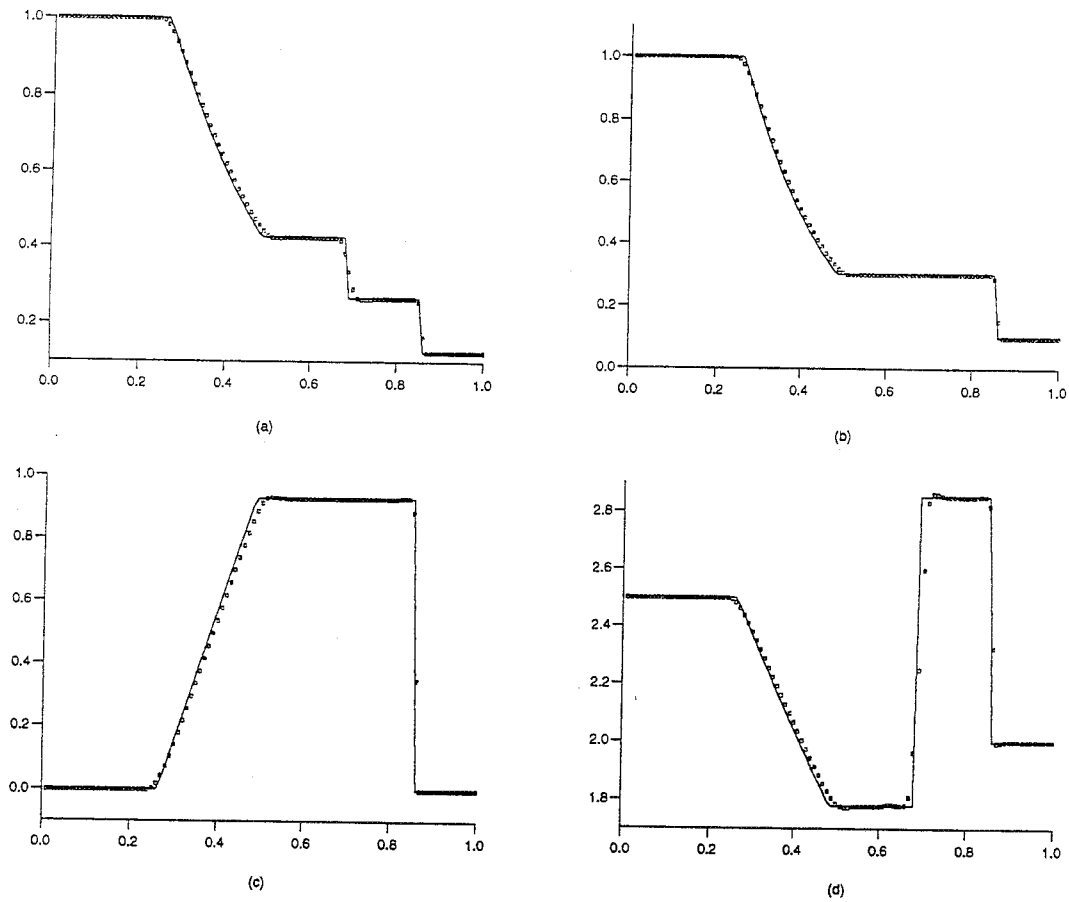

Figure 5: Sod's Problem by the third-order Scheme with the FD3A Limiter: (a) Density, (b) Pressure, (c) Velocity, (d) Energy

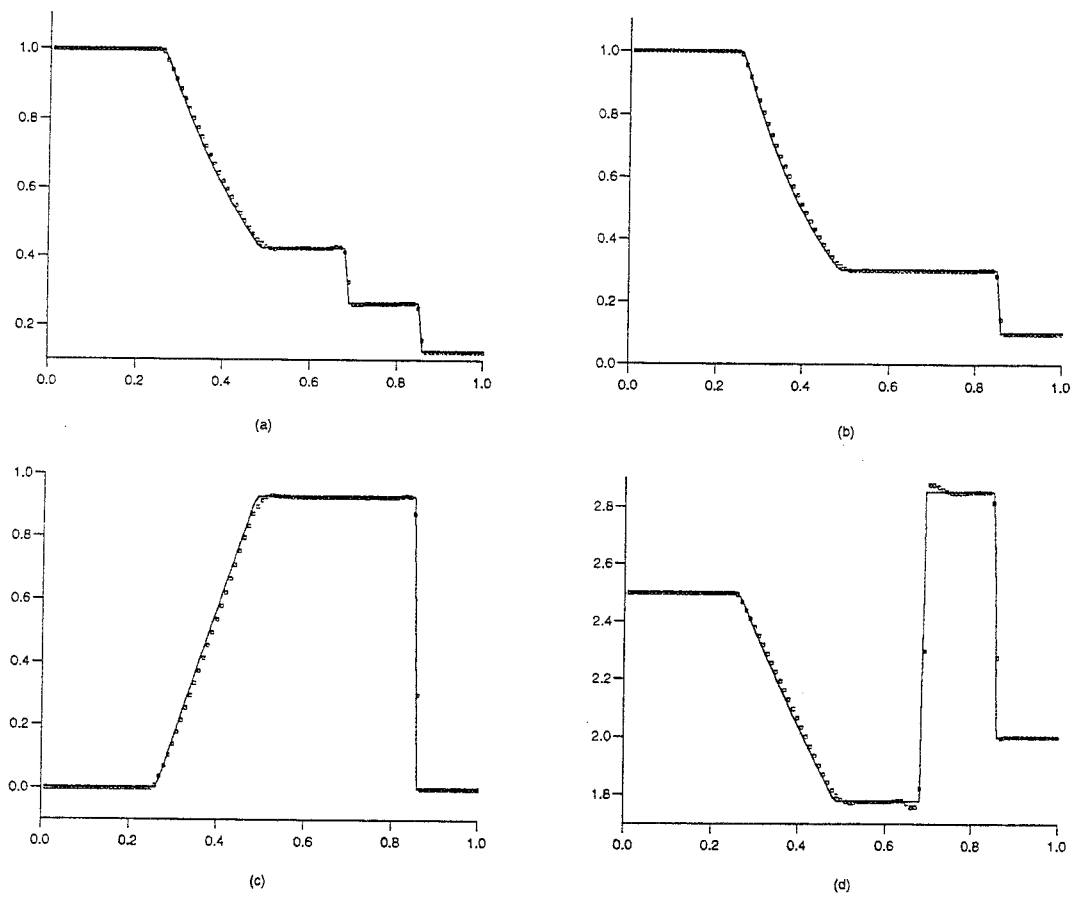

Figure 6: Sod's Problem by the third-order Scheme with the FD3B Limiter: (a) Density, (b) Pressure, (c) Velocity, (d) Energy

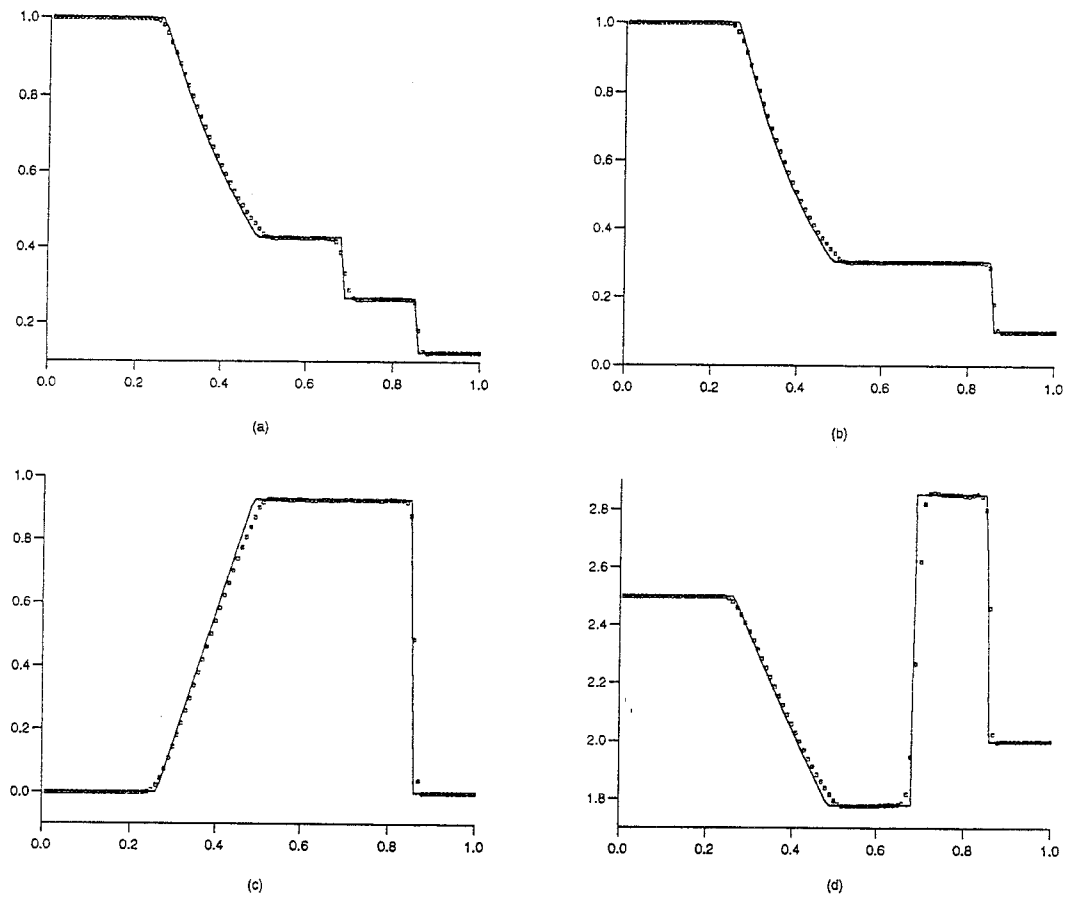

Figure 7: Sod's Problem by the fourth-order Scheme with the FD4A Limiter: (a) Density, (b) Pressure, (c) Velocity, (d) Energy

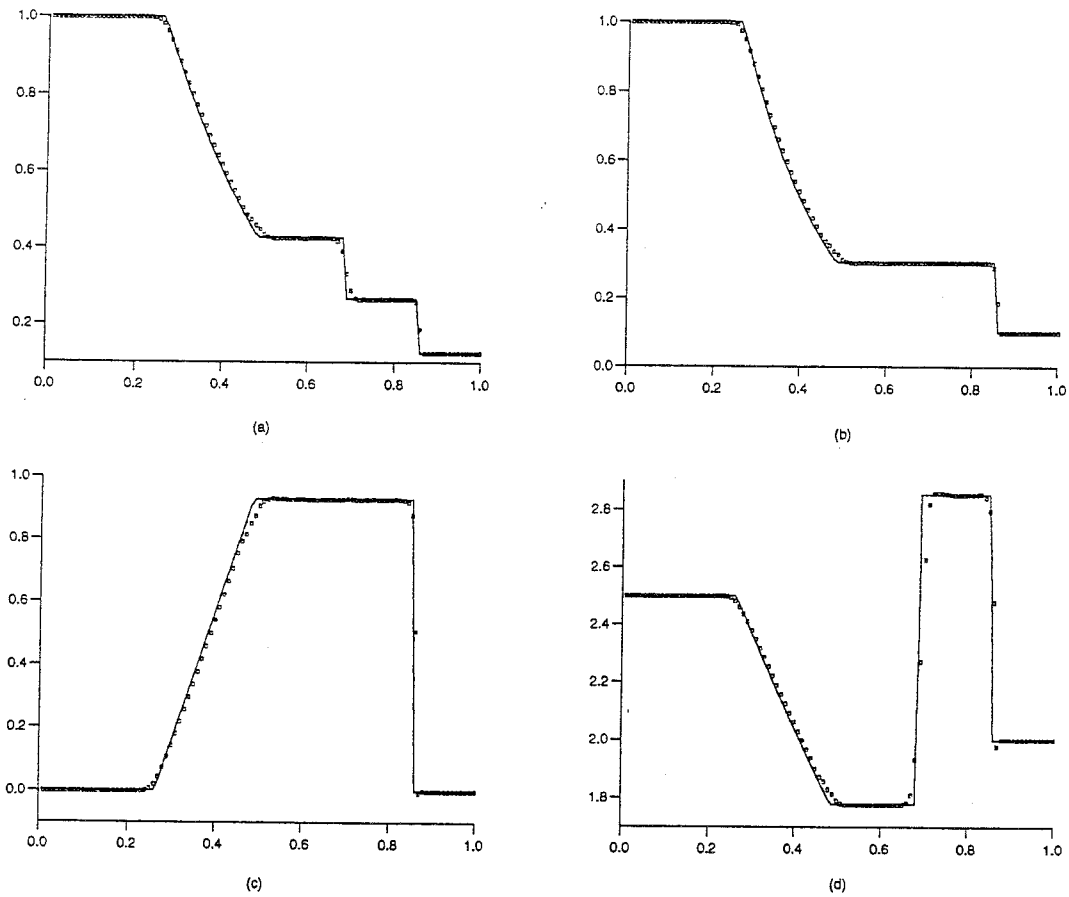

Figure 8: Sod's Problem by the fourth-order Scheme with the FD4B Limiter: (a) Density, (b) Pressure, (c) Velocity, (d) Energy

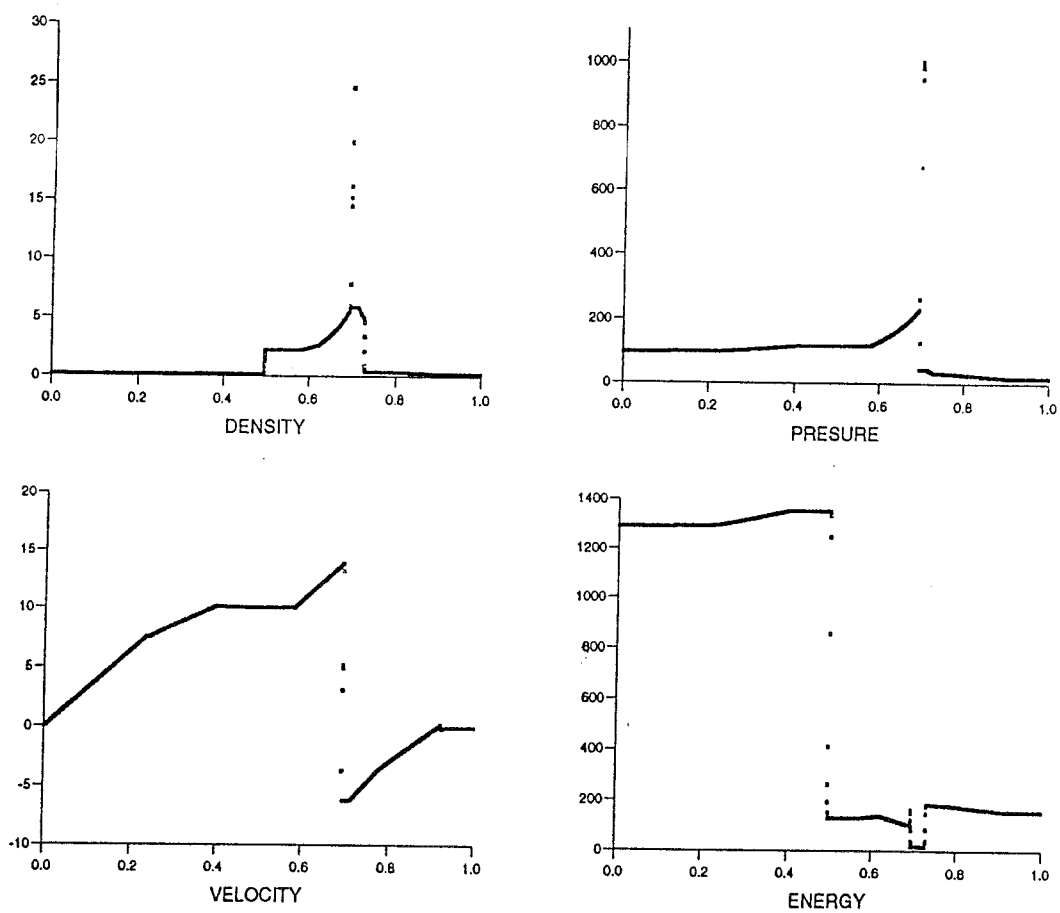

Figure 9: Blast-wave Problem by the Second-order Scheme with the FD2B Limiter

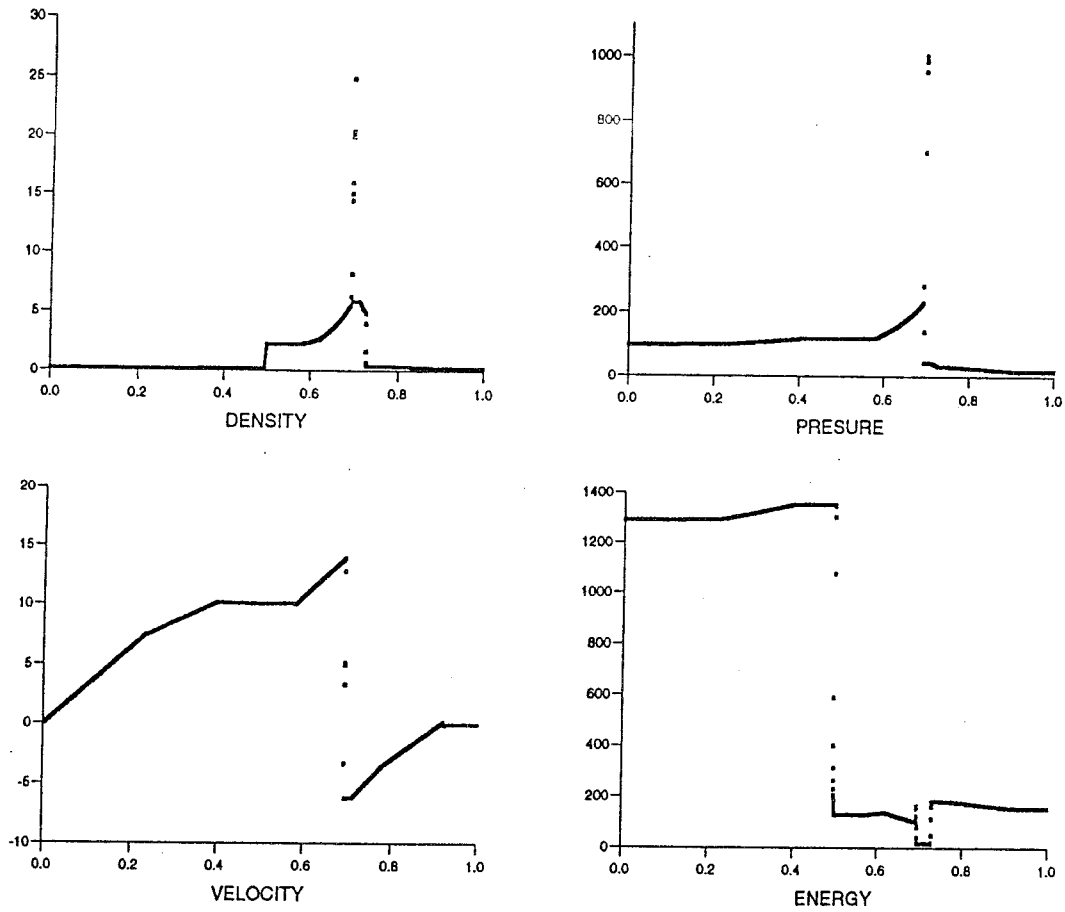

Figure 10: Blast-wave Problem by the Third-order Scheme with the FD3B Limiter

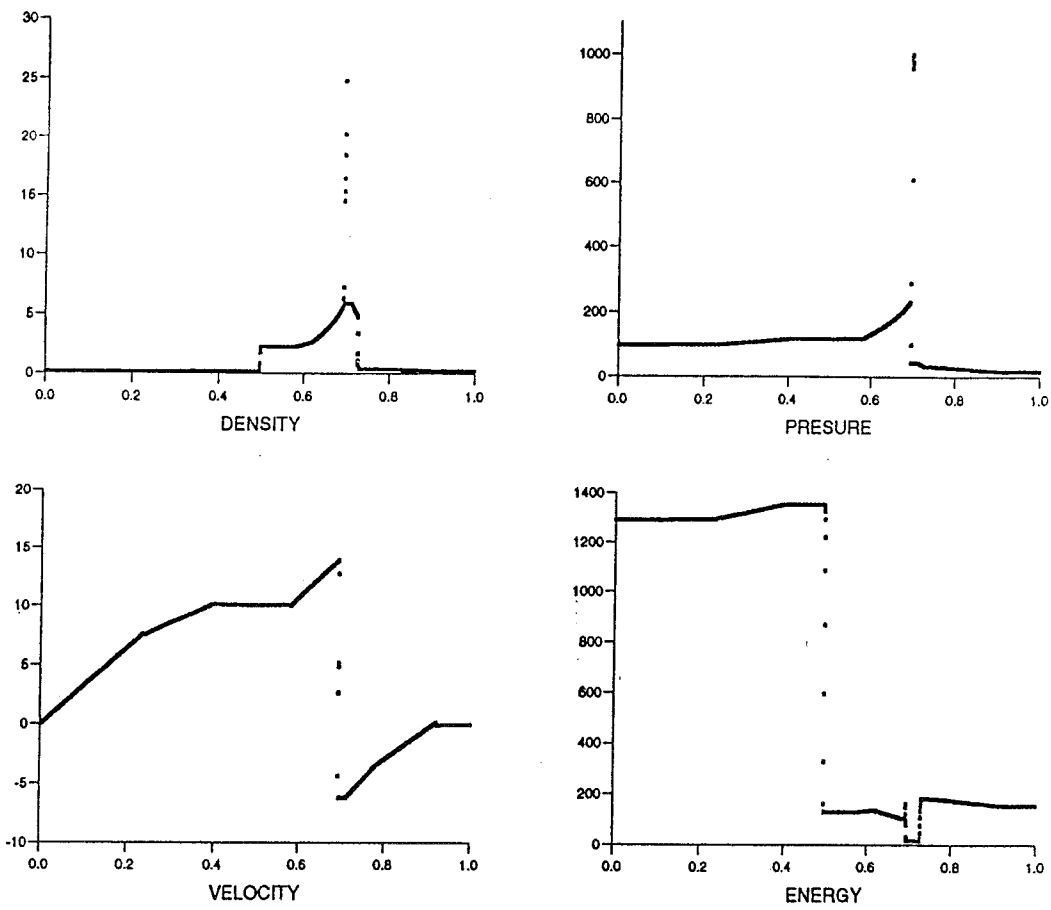

Figure 11: Blast-wave Problem by the Fourth-order Scheme with the FD4B Limiter

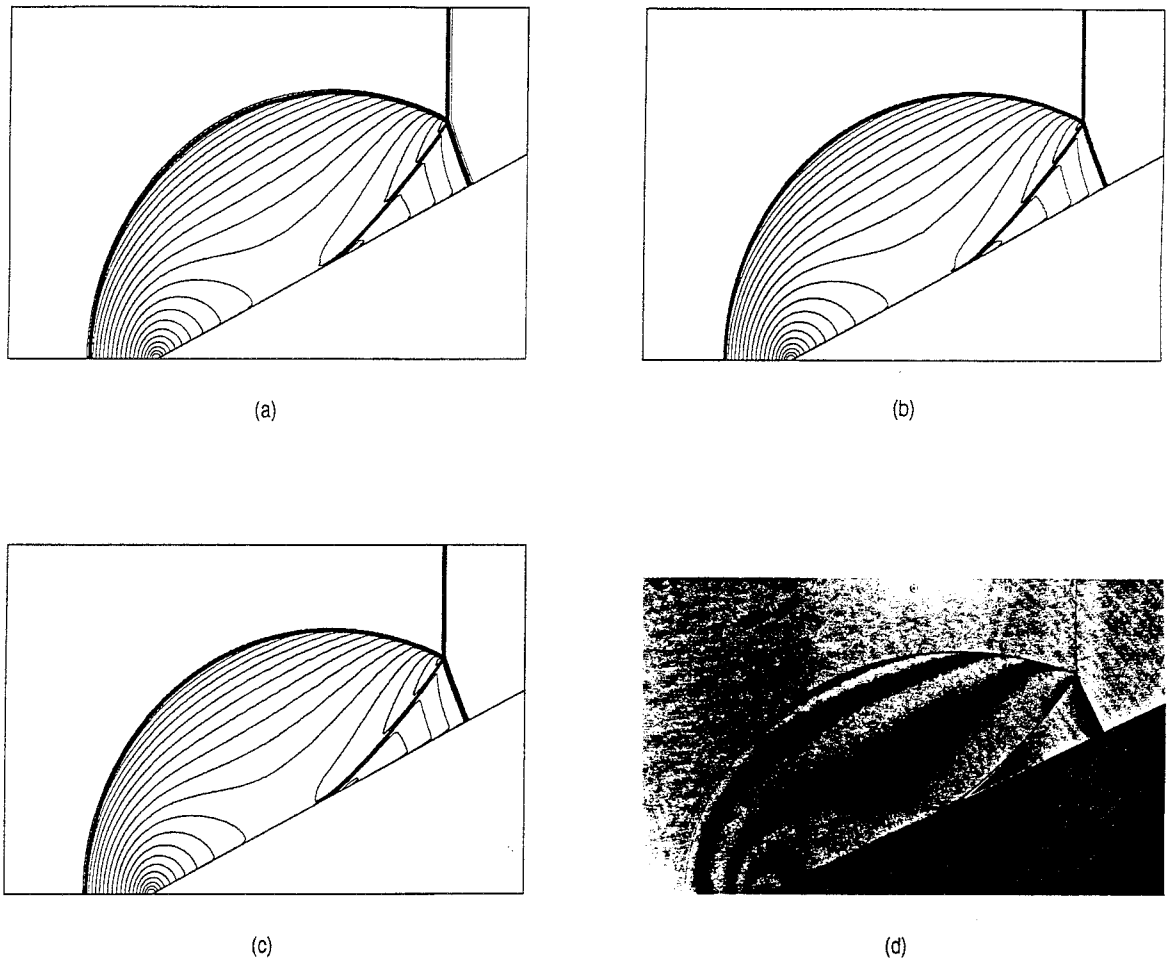

Figure 12: Shock Reflection over 25 Degree Wedge: (a) Computed Result by the Second-order Scheme with the FD2A Limiter, (b) Computed Result by the Third-order Scheme with the FD3A Limiter, (c) Computed Result by the Fourth-order Scheme with the FD4A Limiter, (d) The Experimental Result